Design: Three epithelioid MPNSTs and a tissue array of 68 MPNSTs including 1 additional epithelioid MPNST were examined. Immunohistochemistry was performed by the avidin-biotin-peroxidase complex technique using commercially available antibodies to the following antigens: S-100, HMB-45, tyrosinase, MelanA, and microphthalmia transcription factor (MITF).
Results: All epithelioid MPNSTs were diffusely and strongly positive for S-100. Three of four epitheloid MPNSTs had at least focal melanocytic differentiation (MelanA (2/5), HMB-45 (1/5), tyrosinase (1/5), MITF (0/3). Immunoreactivity was focal in two of the three postive cases while the other positive case exhibited diffuse immunoreactivity. The case with diffuse immunoreacitivity arose within the abdomen of a a 66 year old man. Histologically, it had an extensive epithelioid and spindle cell component and also contained areas of heterologous rhabdomyosarcomatous differentiation (desmin and myogenin positive). While the epithelioid component was diffusely and strongly positive for melanocytic markers, the spindle cell component was negative. All conventional (spindle cell) MPNSTs were negative for all melanocytic markers.
Conclusions: Although very rare, epithelioid MPNSTs can exhibit prominent melanocytic differentiation. This might be related to the ability of neural crest to give rise to both nerve sheath and melanocytic lineages. Epithelioid MPNSTs with melanocytic differentiation may be part of a spectrum of nerve sheath neoplasms with melanocytic differentiation including melanotic schwannomas. Distinguishing epithelioid MPNST with nelanocytic differentiation from metastatic melanoma is best done by identifying origin from a peripheral nerve or helpful histologic features such as areas of heterologous differentiation.

1338 Expression of the Polycomb-Group Protein Bmi1 in Astrocytic Tumors. An Immunohistochemical Study on 80 Cases

R Tirabosco, G De Maglio, M Skrap, G Falconieri, S Pizzolitto. Udine General Hospital, Udine, Italy.
Background: Polycomb-group (PcG) proteins form chromatin-associated complexes involved in epigenetic silencing of some developmental and cell-cycle regulatory genes. These proteins participate in stem-cell self-renewal and thus are expressed throughout life. Bmi1 protein, one PcG member, has a role in hematopoiesis and skeletal and central nervous system development, and its deregulated expression has been implicated in developmental syndromes and experimental cancers, mainly lymphomas. Bmi1 is an inhibitor of INK4a *locus*, a cell-cycle controller via p16 expression, and its possible role in human tumorigenesis is now under investigation. Data are available for lymphomas and breast, lung and colon cancers; however, the function of Bmi1 in brain tumors is underreported. The aim of this study was to assess Bmi1/p16 expression in a large series of gliomas and to evaluate its role in brain tumorigenesis as well as its potential prognostic meaning.
Design: Eighty primary gliomas were evaluated including 16 diffuse astrocytomas grade II (13 fibrillary, 3 gemistocytic), 15 anaplastic astrocytomas grade III and 49 astrocytomas grade IV (glioblastoma, gliosarcoma). Standard immunohistochemistry was applied on paraffin sections using monoclonal antibodies against Bmi1 and p16. Additional stains were done for GFAP, p53 and Ki67.
Results: All tumors, regardless of grade, were diffusely Bmi1 positive. Both Bmi1 and p16 were strongly and diffusely expressed in gemistocytic astrocytomas grade II and in grade III and grade IV astrocytomas with a significant gemistocytic component or a high nuclear grade. On the other hand, p16 was expressed in only 23%, 20% and 22% of fibrillary astrocytomas and in astrocytomas grade III and grade IV, respectively. No association was observed between Bmi1/p16 expression and glial differentiation (GFAP) or p53 and Ki67/MIB1 stains.
Conclusions: Our study shows that the expected Bmi1+/p16- pattern was present in > 75% of tested neoplasms, supporting the current experimental views of its potential role in glioma genesis. Nevertheless, its usefulness as prognostic factor appears questionable, being expressed in all gliomas, regardless of grade. The confusing double expression observed in gemistocytes is in keeping with the intriguing biology of these cells, thought to be terminally differentiated, nonproliferative cells entailing a worse prognosis. Interestingly, the same expression pattern was present in high-grade astrocytomas with gemistocytic component or very anaplastic features.

1339 Immunohistochemical Staining for Peripheral Benzodiazepine Receptors in the Differential Diagnosis of Low Grade Astrocytoma and Reactive Gliosis

E Vlodavsky, M Gavish, JF Soustiel. Rambam Medical Center, Haifa, Israel; The Faculty of Medicine Technion, Haifa, Israel.
Background: The differential diagnosis of low grade astrocytoma and reactive gliosis can be a challenging problem in surgical neuropathology in the era of stereotactic and navigation-guided biopsies, usually yielding small tissue samples. Numerous criteria for differential diagnosis have been proposed, including Ki67 labeling index, p53 staining, etc. These are not very helpful and demonstrate significant overlap between gliosis and astrocytoma. Peripheral benzodiazepine receptor (PBR) is a component of a multiprotein complex located on the contact site between inner and outer mitochondrial membranes. PBR is found in various peripheral organs and glial cells of the central nervous system. The function of PBR in the glia is not clear, but it has been established that PBR expression is significantly increased in 'activated' reactive astrocytes in neurodegenerative, inflammatory and demyelinative diseases. We proposed that immunohistochemical staining for PBR could be useful in differentiating reactive gliosis from low grade astrocytoma.
Design: Paraffin sections from 35 cases of astrocytoma (WHO grades I and II) and 25 cases of reactive gliosis (caused by brain metastases, craniopharyngiomas, pineocytomas, demyelinative lesions and post-radiation gliosis) were stained for Ki-67, p53 and PBR.
Results: Both Ki-67 labeling index and p53 expression demonstrated no significant differences in the cases of gliosis and gliomas. However, immunohistochemical staining for PBR demonstrated striking differences in gliomas and gliosis. Most astrocytomas showed negative results on PBR staining, while weak focal staining was observed in three cases only. In all the cases of reactive gliosis, strong to moderate cytoplasmic staining for PBR was seen. This difference was even more striking in cases of gliosis with pilocytes and Rosenthal fibers vs. pilocytic astrocytoma and gliosis with gemistocytes vs. gemistocytic astrocytoma.
Conclusions: According to our results, immunohistochemical staining for PBR provided a useful clue for differentiating between low grade astrocytomas and reactive astrogliosis, especially helpful in small samples of tissue.

Pathobiology

1340 Refractory ITP: Therapy-Related Histopathologic Changes in Spleens

S Allen, R Chiu, L Baldridge, A Orazi, CH Dunphy, DP O'Malley. Indiana University, Indianapolis, IN; University of North Carolina, Chapel Hill, NC.
Background: Immune thrombocytopenic purpura (ITP) is a common disorder characterized by antibody-mediated destruction of platelets. Refractory ITP (rITP) is a chronic variant characterized by lack of response to the common therapies (e.g. corticosteroids). However, numerous newer therapies have become more widely used before splenectomy, including anti-CD20 antibodies (e.g. rituximab). Few reports exist on the histopathologic changes associate with rITP. We evaluated the splenic histologic and immunohistochemical changes in rITP after a variety of therapies.
Design: 24 cases were reviewed from two institutions including histology and historical information on types of pre-splenectomy therapy. A panel of immunohistochemical (IHC) stains was performed (CD3, CD20, CD79a, PAX-5, CD8, CD68, CD21 and Ki-67). Histology was reviewed for changes in the red pulp, white pulp and vasculature. The results were scored semi-quantitatively (0-3+). Patient groups were defined as follows: Group 1 – conventional therapy (corticosteroids), Group 2 – corticosteroids + additional therapies (IVIG, Rh immune globulin, danazol, cyclophosphamide/ vincristine, rituximab), Group 2A (rituximab alone or with any other therapy). Results were compared using student T-test.
Results: The average ages (age range) were: Group 1 – 43 years (28-63); Group 2 – 49 years (13-79); Group 2A – 69 years (62-72). No statistically significant differences were identified between the histologic or IHC findings of Group 1 (conventional therapy) and Group 2. There were significant differences between Group 2 and Group 2A (rituximab). As expected, CD20 was decreased in both red and white pulp ($P < 0.01$, < 0.001). In addition, CD21 staining was decreased ($P < 0.001$) and CD8 positivity (seen in splenic cords) was increased ($P < 0.05$). This latter measure was inversely related to the number of macrophages. The use of CD79a and/or PAX-5 did not improve detection of B cells in cases with rituximab therapy. Marginal zone hyperplasia was seen in 14/24 cases; extramedullary hematopoiesis was seen in 5/24 cases.
Conclusions: The histopathologic changes seen in post-treatment spleens of rITP are broad with only few characteristic changes seen after specific therapy combinations. The use of rituximab markedly decreases B cells in rITP spleens, consistent with its known effects. It is likely that future treatment modalities will also modify the cellular composition of post-treatment spleens.

1341 Adenosine A2a Receptor in Bone Marrow Derived-Hematopoietic Cells Protects Liver from Ischemia/Reperfusion Injury

F Askarian, D Xu, L Yu, J Chen. Boston University School of Medicine, Boston, MA.
Background: Adenosine A2a receptor (A2aR) is critical in the regulation of inflammatory responses. It has been shown that inflammatory stimulation, which causes minimal damage in normal mice, leads to extensive tissue damage in A2aR-deficient mice (KO) or normal mice (WT) treated with A2aR antagonists.On the other hand, the activation of A2aR protects mice liver from ischemic injury during reperfusion. Since A2aRs express at high levels in hematopoietic cells, such as granulocytes, we hypothesize that A2aR in bone marrow (BM) derived-cells may serve as a major anti-inflammatory mediator in ischemic liver injury.
Design: WT mice, in which the A2aR in BM-derived cells were selectively removed and reconstituted, were generated by transplantation of BM cells from either A2aR-KO mice (KO→WT) or WT mice (WT→WT) following irradiation. Repopulation efficiency of BM-derived hematopoietic cells in the recipient mice was determined by sex chromosome evaluation. Warm liver ischemia/reperfusion was created by clamping the hepatic artery, portal vein and bile duct for 60 min, followed by reperfusion for 23 hours. At the end of the reperfusion, the liver tissues were collected for histological examination as well as RNA isolation. Statistical analysis was performed using student t test.
Results: The microscopic examination of the liver tissues (H & E section) revealed a confluent coagulative necrosis in KO→WT mice. On the other hand, only small foci of necrosis and areas of ballooning degeneration were observed in the WT→WT mice. Neutrophilic infiltration was present in the necrotic areas in both KO→WT and WT→WT mice. However, a majority of neutrophils in KO→WT mice lack A2aR by immunohistochemical study using anti-A2aRs antibody. This result is comparable to the sex chromosome analysis, which demonstrated that approximately 90% of the peripheral blood cells in recipient mice were reconstituted by BM cells from the donor mice. Quantitative real time PCR analysis showed significantly elevated mRNA levels for proinflammatory cytokines, IL-1 and IL-6, in KO→WT mice compared to WT→WT mice.
Conclusions: Adenosine A2a receptor in bone marrow derived-hematopoietic cells protects mouse liver from ischemia/reperfusion injury. This is likely due to inhibition of proinflammatory cytokine production in neutrophils and/or hepatic Kuppfer cells through A2aR-mediated anti-inflammatory mechanism.

1342 "Separation Artefact" *V* Lymphovascular Invasion: Are Mimics Only Mimics?

SH Barsky, Y Ye, NJ Karlin. The Ohio State University College of Medicine, Columbus, OH; Olive View, Sylmar, CA.

Background: Separation artefact (SA), the appearance of tumor clumps within empty tissue spaces is thought to be a tissue artefact of no significance. SA, however, often mimics the appearance of tumor lymphovascular invasion (LVI), a finding of great clinicopathological significance. Because recent experimental evidence has suggested that LVI my evolve from tumor-induced lymphovasculogenesis where endothelial cells form from mesenchymal stem cell precursors and grow circumferentially around the tumor cell clumps, we wondered whether SA might, in fact, be an early stage of LVI and therefore of similar prognostic significance.

Design: 3 groups of 100 cases each of infiltrating ductal carcinomas of the breast stratified for patient age, tumor size, lymph node and ER status were studied and compared with their disease free survival (DFS) and overall survival (OS) statistics. The first group consisted of cases showing SA but no LVI. The second group consisted of cases showing LVI.The third group consisted of cases showing islands of infiltrating ductal carcinoma without either SA or LVI. Cases from each group were subjected to laser capture microdissection. 1000 tumor cell clusters and surrounding extracellular matrix from each case were dissected out and pooled. RNA extraction and RT-PCR were carried out using the appropriate primers for the following angiogenic factor and receptor genes: VEGF, bFGF, Ang-1, Ang-2, Flk-1, Flt-1, Tie-1, Tie-2 and CD31.

Results: The RT-PCR expression profile of the group showing SA strongly resembled the expression profile of the group showing LVI. Specifically both groups showed high expression of VEGF, bFGF, Ang-1, Ang-2, Flk-1, Flt-1, Tie-1 and Tie-2. CD31 expression, however, was absent in the SA group but present in the LVI group. In contrast, the third group lacking SA and LVI showed lower levels of VEGF and bFGF and absent Ang-1, Ang-2, Flk-1, Flt-1, Tie-1, Tie-2 and CD31. Both by univariate and multivariate analysis, SA and LVI showed similarly strongly negative correlations with DFS and OS.

Conclusions: The similar expression profile of angiogenic factors and their corresponding receptors in both the SA and LVI groups together with their similarly strongly negative predictive value for OS and DFS suggests that SA may not be an artefact at all but rather an early stage of LVI. SA may signify a stage where the tumor cell clumps have stimulated lymphovasculogenesis but an earlier stage where the conversion of the mesenchymal cell to the endothelial cell has not yet been completed.

1343 Contributions of Somatic Mismatch Repair Defects to a Differential Microsatellite Profile of MEN 2A C-Cell and Adrenal Medullary Hyperplasias

A Blanes, JJ Sanchez-Carrillo, SJ Diaz-Cano. University of Malaga School of Medicine, Malaga, Spain; King's College Hospital, London, United Kingdom.

Background: C-cell hyperplasias (CCH) and adrenal medullary hyperplasias (AMH) have been reported genetically heterogeneous in multiple endocrine neoplasia 2A. The contribution of DNA mismatch repair to this profile remains unknown.

Design: Microdissected samples from 22 CCH foci and 34 AMH nodules were selected for loss of heterozygosity and single nucleotide polymorphism analyses. Five polymorphic DNA regions from TP53, RB1, WT1, and NF1 were systematically studied by polymerase chain reaction-denaturing gradient gel electrophoresis. Ki-67 (proliferation) and in situ end labeling (ISEL, apoptosis) and kinetic (MIB-1/ISEL) indices were calculated in each sample. Mismatch repair was assessed by MLH1 and MSH2 sequencing and immunostaining in lesions with ≥2 abnormal microsatellite loci (microsatellite instability-high) and in lesions from a sex and age matched control group (11 foci with ≤1 abnormal microsatellite). Only informative cases were included in the final analysis.

Results: The microsatellite analysis showed microsatellite abnormalities for TP53 (12/20, 60%), RB1 (8/14, 57%) in CCH. In contrast, AMH revealed heterogeneous and lower incidence of microsatellite abnormalities for TP53 (9/31, 29%), RB1 (3/25, 12%), WT1 (9/28, 32%), and NF1 (9/19, 47%). Coexistent microsatellite abnormalities in at least two loci (microsatellite instability-high) were observed in 11 samples (20%, 5 CCH and 6 AMH), always involving TP53 in CCH and NF1 in AMH. A significant decrease of MLH1 or MSH2 protein expression with no gene mutations was identified in lesions with high microsatellite instability. The kinetic index of lesions was significantly higher in lesions with microsatellite instability-high (261.25) than in lesions with no or one abnormal microsatellite (169.38), due to a significantly lower ISEL index.

Conclusions: 1. Somatic down-regulation of mismatch repair proteins contributes to both the accumulation of microsatellite lesions and genetic heterogeneity in MEN 2A lesions, resulting in a differential microsatellite profile (predominating TP53 in CCH and NF1 in AMH). 2. MEN 2A genetically instable lesions reveal the most advantageous kinetic profile, essentially due to down-regulated apoptosis.

1344 Slit2 Expression in Human Neoplasms: A Preliminary Tissue Microarray Study of 839 Cases

N Chen, XQ Chen, J Gong, B Yang, YT He, W Yin, XL Liu, XJ Wang, Q Zhou. West China Hospital, West China Medical School, Sichuan University, Chengdu, Sichuan, China.

Background: Slit2, a member of the recently identified Slit protein family, function as chemorepellent of neuronal migration and inhibitor of leukocyte migration, via cellular signalling through binding to the Roundabout (Robo) receptors. Recently, Slit2 was reported to be overexpressed in several cancer cell lines and cancer tissues. Slit2 appeared to be involved in tumor angiogenesis through Slit-Robo interaction and the PI3K pathway.

Design: Expression of Slit2 protein was evaluated by immunohistochemistry with a monoclonal antibody (gift of Dr. J. Geng, University of Minnesota) in 839 tissue samples using tissue microarrays (TMAs). The TMAs were constructed as described by Chen and Zhou (Am J Clin Pathol, 124:103), and included the following tumors: esophageal squamous carcinoma (164 cases), gastric adenocarcinoma (115), colorectal adenocarcinoma(207), hepatocellular carcinoma (49), adenocarcinoma (62) and squamous carcinoma (70) of the lungs, various types of soft tissue sarcomas (113), lymphoblastic lymphomas (18) and diffuse large B cell lymphomas (41).

Results: Moderate to strong reactivity for Slit2 was observed in 36.5-59.2% of gastrointestinal adenocarcinomas and hepatocellular carcinomas. Positivity in squamous carcinomas was much lower (8.6-12.8%) and weaker. The sarcomas and lymphomas lacked reactivity with this antibody, except for focal staining in synovial sarcomas and clear cell sarcomas. Our preliminary data did not reveal significant correlation between Slit2 expression and tumor grade, stage, and patient survival. A more comprehensive study is underway for better understanding of this molecule.

Conclusions: Slit2 appeared to be preferentially expressed in carcinomas, notably adenocarcinomas, but was absent in most sarcomas and lymphomas. These data indicate that Slit2 might serve as a potential immunomarker for a subset of human neoplasms, particularly glandular epithelial cancers.

1345 Expression of Peroxisome Proliferator Activated Receptor Gamma (PPAR-γ) in Pancreatic Ductal Adenocarcinoma (PDAC) and Pancreatic Intraepithelial Neoplasia (PanIN)

Y Dancer, M Moghadamfalahi, J Thibodeaux, J Albores-Saavedra. The Methodist Hospital, Houston, TX; Lousiana State University, Shreveport, LA.

Background: The peroxisome proliferator activated receptors (PPARs) are ligand – dependent transcription factors which belong to a nuclear hormone superfamily. PPAR-γ has been shown to participate in growth inhibition and differentiation in several cancers. In the pancreas, PPAR-γ and its agonists have been proposed to act as tumor suppressors and possibly differentiation factors. The role of PPAR-γ in normal differentiation and in tumorigenesis is unknown. Past studies have revealed that PanINs accumulate clonal genetic changes, showing that they are precursors of ductal adenocarcinomas. In this study, we evaluated expression patterns of PPAR-γ in the progression of PanIN to PDAC.

Design: 28 surgically resected specimens with PDAC were reviewed and the most representative paraffin-embedded blocks were chosen for further analysis. Clinicopathologic characteristics, which included age, tumor size and AJCC stage were evaluated. The median age of the patients at the time of operation was 64 years (range 34-82). Immunostaining with PPAR-γ (mouse monoclonal antibody, Santa Cruz, CA) was performed on the study specimens. Results were graded as positive if more than 10 percent of cells showed staining. In the positive cases, the staining patterns were assessed by two pathologists using light microscopy. Chi -Square analysis and the Student T Test were used to generate the statistical data.

Results: Sixteen of twenty eight cases (57.2%) were positive for PPAR-γ . The mean ages were 63 ± 8.39 in the PPAR-γ positive group vs. 64.14 ± 15.37 in the negative group ($p>0.05$). Tumor sizes were 3.56 ±1.01 vs. 2.64 ±1.00 ($p>0.05$). Only cytoplasmic staining was observed in normal ductal epithelium. Weak to moderate staining was observed in PanIN. Both cytoplasmic and nuclear staining was observed (60% cytoplasmic and 40% nuclear). In the invasive component of PDAC , staining was predominantly nuclear. The nuclear staining was from moderate to strong intensity.

Conclusions: PPAR-γ expression was confined to the cytoplasm of normal ductal epithelial cells in our study. We demonstrated low nuclear expression of PPAR-γ in precancerous lesions and high nuclear expression of PPAR-γ in PDAC. Our data suggests PPAR-γ might be involved in the progression of PanIN to PDAC.

1346 Identifying Genes that Regulate Organogenesis: A Gene-Trap Approach in Zebrafish

JM Davison, SD Leach, MJ Parsons. Johns Hopkins Medical Institutes, Baltimore, MD.

Background: Organogenesis is the tightly orchestrated process by which embryonic primordia develop into fully-differentiated and functional organs. In the context of the adult organ, genes which play a role in organogenesis and embryo patterning are utilized for such vital homeostatic processes as tissue maintenance, renewal and regeneration after injury; their function is altered in many human disease states ranging from genetic syndromes to cancer. The zebrafish (*Danio rerio*) is an ideal model vertebrate organism in which to study organogenesis: the developing zebrafish is transparent, allowing one to visualize developing organs; many zebrafish organs exhibit striking histologic similarity to human tissues; and zebrafish are small enough to be used in forward genetic screens. We have designed a novel "gene-trap" screen in zebrafish to identify genes which are expressed in developing organs and to study their function.

Design: The Tol2 transposon has been engineered to carry a gene-trap construct (fig. 1A). This plasmid construct is injected with Tol2 transposase mRNA into single-cell zebrafish embryos. The transposase enzyme catalyzes the transposition of the vector from the donor plasmid to random sites throughout the genome. Injected fish are bred with wild-type zebrafish to obtain F1 embryos which are screened for GFP expression. GFP is expressed under the control of the "trapped" gene's regulatory elements when the construct transposes into the transcribed portion of a gene (fig. 1A). The gene trap vector is potentially mutagenic because it disrupts exon splicing and open reading frames.

Results: Over twenty distinct GFP expression patterns have been observed in F1 embryos from the initially injected F0 founders. Two such patterns are illustrated (fig. 1B).

Conclusions: Our gene-trap approach has been utilized to identify regions of the genome harboring genes which are expressed during organogenesis. We are currently raising these F1 embryos and work has begun in order to identify the loci harboring inserts. Also, transgenic lines expressing Gal4VP16 in tissue specific patterns are being raised.

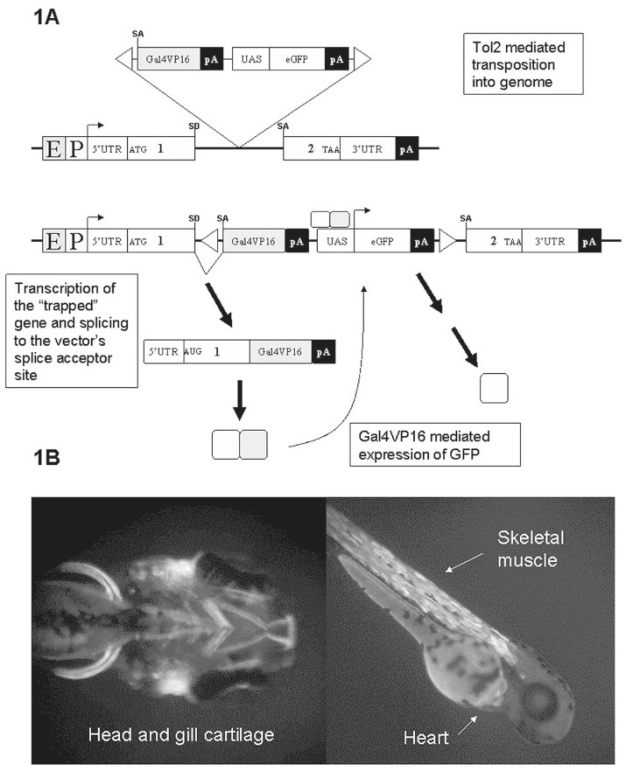

1347 Diagnostic Value of D2-40 in Separating Metastatic Seminoma from Other Metastatic Malignancies

C Deng, YL Liu, RS Saad, SS Shen, Q Cai, JF Silverman. Allegheny General Hospital, Pittsburgh, PA; The Methodist Hospital, Houston, TX.

Background: The cytomorphologic and histologic features of seminoma overlap with those of malignant lymphoma, melanoma, poorly differentiated carcinoma and small round blue cell tumors. Therefore, immunohistochemical studies are often obtained in the working-up metastatic malignancy of unknown origin when these diagnoses are entertained. M2A, an oncofetal protein associated with a germ cell line, has been found in the fetal gonocytes, intratubular germ cell neoplasia, and germ cell tumor. D2-40 is a monoclonal antibody against M2A and has been shown to be expressed in seminoma. However, the diagnostic value of D2-40 in separating metastatic seminoma from other metastatic malignancies of unknown origin has not been investigated.

Design: Total 60 cases including 15 seminoma, 15 metastatic malignant melanoma, 15 maligant lymphoma and 15 poorly differentiated carcinoma were retrieved from the department data base. The immunostaining of paraffin sections for D2-40 was performed on an automated immunostainer using biotin-avidin-complex method with appropriate positive and negative controls.

Results: Positive D2-40 immunoreactivity was seen in all the seminomas and 1/15 metastatic poorly differentiated carcinoma. No immunoreactivity was observed in the neoplastic cells of the malignant lymphomas and metastatic melanomas.

Conclusions: Our results indicate that D2-40 is a highly sensitive immunohistochemical marker for seminoma. Therefore, D2-40 should be included into the immunohistochemical panel for the work up metastatic malignany of unknown origin when the differential diagnosis includes seminoma, malignant melanoma, malignant lymphoma and metastatic poorly differentiated carcinoma.

1348 Lymphatic Vessels Distribution in Normal Colonic Mucosa, Adenomatous Polyps and Colorectal Carcinomas Using the Novel Immunostaining

KL Denning, RS Saad, YL Liu, L Kordunsky, JF Silverman. Allegheny General Hospital, Pittsburgh, PA.

Background: Electron microscopy has previously been used to evaluate the distribution of lymphatic vessels in normal and neoplastic colon due to the lack of a specific immunohistochemical lymphatic marker. Previous studies have demonstrated that lymphatic vessels are distributed beneath the muscularis mucosae with only rare branches reaching through the muscularis mucosae to the most basal aspect of the colonic crypts. Therefore, the colonic lamina propria is believed to be essentially devoid of lymphatics. Recently, D2-40, a novel monoclonal antibody, is available as a specific lymphatic marker. In this study, we analyzed the distribution of lymphatic vessels in normal colon, adenomas and invasive carcinomas using D2-40 immunohistochemical (IHC) marker.

Design: A total of 100 cases, including 25 normal colonic mucosa, 10 hyperplastic polyps, 10 tubular adenomas, 15 villous adenomas, and 40 adenocarcinomas of the colon (10 cases pT1, 10 cases pT2, 10 cases pT3 and 10 cases pT4) were retrieved from the hospital database. Immunostaining with antibodies to D2-40 and CD34 were performed on paraffin-embedded tissue. Immunostain were performed on an automated immunostainer with appropriate positive and negative controls. Two pathologists screened the cases for D2-40 stained lymphatic vessels.

Results: In normal colonic mucosa, D2-40 showed lymphatic vessels distributed beneath and above the muscularis mucosa in the deep lamina propria in all the normal colonic mucosa evaluated. Hyperplastic polyps showed a similar distribution to the normal mucosa. D2-40 identified lymphatic vessels in the superficial lamina propria with increased density in the stalk stroma in the majority of villous adenomas (8/10, 80%) and 4/10 (40%) tubular adenomas. D2-40 stained lymphatic vessels in all 40 (100%) cases of colon adenocarcinoma irrespective of their depth of invasion (T level).

Conclusions: In contrast to previous studies with D2-40 monoclonal antibiodies, lymphatic vessels were identified in the deep lamina propria in normal colonic mucosa. In addition, colonic adenomas (particularly villous adenomas) demonstrated lymphatic vessels in their lamina propria. The presence of lymphatic vessels in the deep lamina propria may explain the rare metastasis in cases having colon carcinoma confined above the muscularis mucosa.

1349 New Vectors for Prostate Cancer Gene Therapy. Expression of Kaposi's Sarcoma-Associated Herpes Virus (KSHV) Cyclin D Homologue, K-Cyclin Exerts a Marked Cytotoxic Effect and Increases Sensitivity to Chemotherapy

M Diaz-Fuertes, J Hernandez-Losa, C Parada, R Sanchez, L Lopez, J Jimenez, S Ramon y Cajal. Vall d´Hebron University Hospital, Barcelona, Spain.

Background: Kaposi's sarcoma-associated herpesvirus (KSHV) cyclin D homologue, K-Cyclin (CK), can act as a potent cell-cycle inductor associating with cellular Cdk4 and 6 to form a kinase complex that phosphorylates and inactivates the retinoblastoma tumour suppressor protein (Rb). These complexes can also induce apoptosis in cells with high levels of CDK6 and *wt*p53. In addition to Rb, K-Cyclin/Cdk complexes can phosphorilate other proteins such as p27Kip and bcl2, inactivating its anti-apoptotic function.The aim of this study is to use a very lethal gene able to kill cells independently from the status of p21, p27 and p16 and that by inactivating bcl2 increases sensitivity to anticancer drugs. To avoid side effects in normal cells we add an androgen dependent promoter (Probasin), which drives K-Cyclin expression only to prostate cells.

Design: CK gene has been cloned into several vectors under the specific control of prostate promoter "Probasin". These constructions have been then transient-transfected into human prostate cell lines (PC3, DU145 and LNCap) and human non-prostate cell lines (A549, Hela, 293T, Ovcar4). Blc2 gene has been stable-transfected in all cell lines tested with specific vectors. The lethal effect of CK under Probasin promoter in combination with chemotherapeutic CDDP (Cisplatin) treatment was finally evaluated in all cell lines over-expressing Bcl2.

Results: Significant cell death due to CK expression under Probasin promoter was observed in two of the three prostate cell lines in study (LNCap and DU145). In the androgen independent cell line PC3 as well as in the non-prostatic cell lines no relevant cytotoxic effect was observed. The same cell lines over-expressing the Bcl2 protein showed enhanced lethal effects after CDDP treatment in combination with CK transfection controlled under Probasin promoter. After three days of treatment with CDDP, over 95% of androgen-dependent cells were killed.

Conclusions: The expression of K-cyclin which kills cells with *wt*p53 and phosphorilates bcl2 showed a high cytotoxic effect and increased the sensitivity to anticancer agents. We proposed the employ of this genetic approach in the treatment of bcl2 overexpressing tumors. The constructs with a specific promoter such as probasine circunscribe the cytotoxic effect to androgen dependent cells.

1350 Evolutionary Relationship of Annexin Genes in Human by Bioinformatics Methods

YI Elshimali, D Chen, C Aoyama, P Liu. Olive View UCLA Medical Center, Sylmar, CA.

Background: Annexins are calcium and phospholipid binding protein, which are evolutionary conserved and expressed from plants to animals. They are reported to be involved in calcium ion regulation, calcium channel and epithelial growth factor receptor (EGFR) phosphorylation as the major substrates. Aberrant expression of annexin genes is identified in different malignancies. In order to conduct a comprehensive evaluation of annexin genes in human for a cancer biomarker discovery project, electronic sequence analysis of annexin genes was performed to determine the evolutionary relationship of annexin genes (finding novel member) in human by bioinformatics methods.

Design: Human and mouse annexin gene mRNA sequences were retrieved from UCSC Genome Browser. Reciprocal best hits were established between human and mouse sequences to determine orthologous gene pairs. Novel annexin sequences in human and mouse were discovered by alignment of existing genes to human and mouse genome sequences. In addition, both human and mouse gene transcripts were electronically mapped to chimpanzee sequences to determine uncharacterized annexin genes. In addition, by using VISTA program, genome sequence comparison of all the characterized annexin gene sequences in both human and mouse were conducted to determine the locations of evolution conserved sequences.

Results: In addition to the 13 characterized human annexin and 10 mouse annexin genes, additional 3 human and 4 mouse uncharacterized annexin genes were identified through our genome alignment efforts. Electronic mapping of human annexin genes to the chimpanzee genome on UCSC genome browser showed complete match, i.e. all 16 human annexin genes mapped to its putative syntenic position on the chimpanzee genome.

Conclusions: Comparison between human and mouse annexin genes revealed 12 orthologous gene pairs. This indicates that 4 human and 5 mouse annexin genes arise from duplication events after the speciation event between human and mouse lineage. The complete annexin gene set in human might have established before the speciation between human and chimpanzee 5 million years ago. Electronic sequence analysis of annexin genes is an effective way to decipher the evolutionary relationship of this important gene family.

1351 Down-Regulation of BCRP/ABCG2 during Tumorigenesis *In Vivo*

AV Herdman, N Gupta, PM Martin, S Miyauchi, H Hu, RG Martindale, R Podolsky, RB Hessler, V Ganapathy. Medical College of Georgia, Augusta, GA; Oregon Health Sciences University, Portland, OR.

Background: Breast Cancer Resistance Protein (BCRP) expression is associated with chemotherapy resistance in cancer, and has recently been shown to confer protection from genotoxins like PhIP by removing them from cells. Thus, BCRP has therapeutic implications. To date the differential expression of BCRP with malignant transformation in human tissue has not been examined. We hypothesized that BCRP was down regulated in cancer.

Design: We examined paired normal and cancer tissues from 13 colorectal cancers (CRC) and 1 hepatic metastasis from a CRC primary for BCRP expression by semi-quantitative RT-PCR, Northern Blot and immunohistochemistry (IHC). Paired normal and cancer cDNA BCRP differential expression was evaluated using a commercial dot blot assay from 154 patients with tumors in 19 different tissues. IHC was used to further study protein expression in 12 tissues that demonstrated a significant down-regulation of mRNA.

Results: BCRP mRNA was present in normal colorectal and hepatic tissue and showed a mean decrease in cancer of 6.6 ± 0.6-fold by RT-PCR ($p<0.0001$) and a mean decrease of 4.9 ± 0.5-fold by Northern blot ($p<0.005$). There was a statistically significant decrease in BCRP mRNA levels in 12 of the 19 different cancer sites. BCRP protein expression was abundant in the normal colon on IHC, and showed a decrease in colon cancer, as well as in each of the organ sites that demonstrated down-regulation on the commercial array.

Conclusions: BCRP is significantly down regulated with malignant transformation in several human tissues. Decreased expression of BCRP may have a role in tumorigenesis via an accumulation of genotoxins.

1352 The Biological and Pathological Fetures of Epstein-Barr Virus(EBV)-Associated Gastric Carcinoma

R Hino, H Uozaki, M Fukayama. Tokyo University, Graduate School of Medicine, Tokyo, Bunkyo-ku, Hongo, Japan.

Background: Epstein-Barr virus(EBV)-associated gastric carcinoma(GC) (EBVaGC) accounts for up to 10 % of all cases of GC and is distributed uniformly worldwide without any regional accumulation. EBV is closely related to the genesis of EBVaGC. However, the developmental process of EBVaGC has not been clearly demonstrated. To clarify the mechanism of the EBVaGC development, we used 6 GC cell lines infected with EBV and compared these cell lines biologicaly, molecular biologicaly and pathologically with 6 EBV-negative GC(EBVnGC) cell lines.

Design: We investigated the difference between 6 EBVaGC cell lines(MKN1,MKN7, MKN74,AGS,NUGC3,TMK1) and 6 EBVnGC cell lines biologicaly(MTT assay, Wounding assay, Invasion assay and TUNEL assay). To clarify the cellular and molecular abnormalities in EBVaGC cell line compared to EBVnGC cell line, we applied the high-density oligonucleotide array analysis(gene chip), a rapid method to scan the differential expression all at once. Real time RT-PCR confirmed the results obtained from the chip hybridization. Further investigations(RNAi, transfection with an individual EBV latent gene expressed in GC and immunohistochemistry) were applied to the gene that showed remarkable difference between those in gene chip and real time RT-PCR.

Results: There were striking differences between EBVaGC and EBVnGC cell lines under serum deprivation condition(MTT assay, Wounding assay, TUNEL assay). On the other hand,there was no difference between those under FCS10%-medium condition.Gene chip analysis revealed that the gene associated with apoptosis, especially survivin, showed markedly higher expression in the EBVaGC cells than in the EBVnGC under serum deprivation.Downregulation of survivin by RNAi remarkably inhibited the growth of EBVaGC cell. Immunohistochemistry revealed 77.8% of EBVaGC were survivin positive.

Conclusions: Survivin is found in most human cancers included gastric carcinoma, and expression of survivin correlated with anti-apoptosis, poor prognosis, and increased risk of recurrence.This is the first report showing that survivin is a key role in resistance against the serum deprivation induced apoptosis in EBVaGC cells. Survivin inhibition therapy may be useful for the treatment of EBVaGC.

1353 Immunosuppressive Alterations in Axillary Sentinel Lymph Nodes in Early Breast Cancer

JR Lee, K Subbannan, A Kallab, DH Munn. Medical College of Georgia, Augusta, GA; Veterans Affairs Medical Center, Augusta, GA.

Background: Host immunotolerance to unique tumor antigens plays a key role in tumor growth and development of metastatic disease. It is known that malignancy draining sentinel nodes (without metastases) demonstrate significant cellular and architectural alterations. Recent discovery of a subset of dendritic cells that initiate T-cell immunotolerance at the time of antigen presentation is felt to be a mechanism of sentinel nodal immunotolerizing alteration (Science 297:1867-1870 (2002)). CD123 positive antigen presenting cells that express the tryptophan degrading enzyme IDO (indolamine 2,3-dioxygenase) have been identified in tumor draining lymph nodes. In a study of melanoma draining lymph nodes, the presence of nodal IDO positive plasmacytoid cells predicted a worse clinical outcome (J Clin Invest 114:280–290 (2004)).

Design: Archival tissues and records of 86 patients with sentinel lymph node dissections for all stages of breast cancer were obtained from the Medical College of Georgia. 13 patients harbored DCIS, 34 patients demonstrated low-grade malignancy (T1N0M0), and 39 patients had high-grade malignancy. IDO immunostaining was performed on 156 sentinel lymph nodes. Grading of nodal IDO involvement was determined by identifying the infiltration percentage of IDO positive cells in the perisinusoidal region of any given node ("normal" = <5%; 1+ = 5-25%; 2+ = 25-50%; 3+ = 50-75%; 4+ = 75-100%). The highest grade was selected as the grade for all removed sentinel node(s) in each case.

Results: 36 sentinel nodes were positive for malignancy in 28 patients (N1 (23 patients); N2 (5 patients)). Four metastatic foci were detected by cytokeratin immunostaining. 44% of cases (38/86) demonstrated >5% IDO staining. Altered sentinel nodes involved with IDO positive cells were identified in 54% of cases with DCIS (7/13), 62% of cases with low grade disease (21/34) and 46% of cases with high grade malignancy (18/39).

Conclusions: Immunotolerant alterations occur within sentinel lymph nodes at an early stage of breast carcinoma development, even before invasive malignancy is detected. It appears that aggressive immunotherapy to block IDO activity may be indicated as an adjunct to adjuvant chemotherapy, even in early mammary malignancy.

1354 Lymphotoxin Pathway Directed, AIRE-Independent Central Tolerance to Arthritogenic Type-II Collagen (CII)

W Liu, RK Chin, M Zhu, Y-X Fu. The University of Chicago, Chicago, IL.

Background: Autoimmune regulator (Aire) drives the presentation of immunological self in the thymus through the ectopic expression of peripherally restricted antigens by thymic medullary epithelial cells (mTEC). Mutations in the Aire gene are responsible for multi-organ autoimmune diseases. The expression of Aire in mTECs is directed by signaling through the lymphotoxin-β receptor. Its ligand lymphotoxin (LT) is upregulated on activated thymocytes. Autoimmune diseases have been documented in LT knockout mice (lta-/- and ltbr-/-). CII is the arthritogenic antigen in the mouse model of rheumatoid arthritis (RA) and collagen induced arthritis (CIA). Given the essential contributions of autoreactive T cells to the pathogenesis of both RA and CIA, we sought to define the role of central tolerance in forestalling anti-CII autoimmunity, and examine the input of both Aire and LT to this process.

Design: Real-time PCR for CII mRNA expression and IHC for CII protein expression were performed in WT, Aire-/-, lta-/- and ltbr-/- thymi. The spontaneous production of anti-CII antibodies in lta-/- and ltbr-/- mice was analyzed by ELISA. Splenocytes from ltbr-/- mice were transferred into irradiated Rag1-/- mice. Thymi from ltbr-/- and WT newborn pups were transplanted under the kidney capsule of the thymectomized B6 mice. Histologic examination of the joints was done.

Results: The ectopic expression of CII in the thymus is present in Aire-/- mice. The significant reduction in CII expression in the thymi of lta-/- and ltbr-/- mice leads to spontaneous anti-collagen autoimmunity, similar to clinical presentation of RA. Rag1-/- recipients of ltbr-/- donor splenocytes were able to recapitulate the findings of lta-/- and ltbr-/- mice. Significant higher levels of anti-CII antibodies in recipients of ltbr-/-thymi were observed. While WT B6 mice remained only mildly symptomatic in response to repeat immunizations, all lta-/- mice developed fulminant disease phenotype after secondary immunization heterologous CII emulsified in CFA

Conclusions: We show here that the ectopic expression of CII in the thymus, and the corresponding central tolerance to CII are AIRE-independent, but lymphotoxin dependent. The failure to express CII in the thymi of lta-/- and ltbr-/- mice leads to overt autoimmunity to CII, and exquisite susceptibility to arthritis. These findings define the existence of additional lymphotoxin directed pathways of ectopic peripheral antigen expression, parallel to and independent of AIRE, which cover an extended spectrum of peripheral antigens.

1355 Mutational Profile of Sentinel Lymph Node Metastasis in Breast Cancer: Pathobiology Implication

YL Liu, X Lin, JF Silverman, RS Saad, SD Finkelstein. Allegheny General Hospital, Pittsburgh, PA; RedPath Integrated Pathology, Inc, Pittsburgh, PA.

Background: Breast cancer (BC) stage is a predictive of disease aggressiveness and survival. Sentinel lymph node (SLN) has assumed a critical role in determining the need for axillary resection and additional therapy. The underlying mechanism for early tumor spread is largely unknown, although it is likely based upon specific mutational changes acquired by each individual BC. We studied SLN spread using a combined histopathologic/molecular approach to gain insights into the heterogeneity of this process.

Design: Five patients with positive SLN and BC were retrieved from the pathology archives. Multiple microscopic tissue targets were microdissected from both primary and SLN for comparative mutational analysis. Aliquots of DNA were analyzed for allelic imbalance (LOH) using PCR/electrophoresis and a panel of 15 polymorphic microsatellite markers targeting 1p,3p,5q,9p,10q,17p,17q,21q,22q. A total of 105 mutational assays were performed. Temporal sequence of mutation acquisition was based on clonal expansion model correlated with topographic distribution and extent of imbalance. Fractional mutation rate (FMR), a measure of cumulative acquired mutations, was defined as the total # mutations/total # informative markers.

Results: BC ranged from 0.9 to 3.5 cm in greatest dimension. FMR ranged from 0.10 to 0.67 without correlation with tumor size supporting that BC can arise as intrinsically aggressive malignancy. The number of SLN removed ranged from 3-13 with 1-5 being positive. The patient with the highest positive SLN rate (5/5, 100%) exhibited the highest FMR while those tumors with the lowest SLN positive rate (1/8, 12.5% 1/13, 7.7%) had the corresponding lowest FMR (0.1, 0.15). Also, the patient with the highest

SLN FMR had the highest number of positive LN (32/35). SLN FMR was lower than primary BC FMR in 3 patients with the lowest number of positive LN, whereas the converse was seen in patients with the highest number of positive LN. A greater concordance in early acquired mutations was present in the patients with highest positive axillary LN status.

Conclusions: By defining and then comparing the mutational profile between primary and SNL metastasis, valuable pathobiologic information concerning the intrinsic aggressiveness of BC is available that can be integrated with the histopathologic features. BC showed progressive mutation accumulation between the primary and metastatic sites may represent aggressive subset of patients with early spread of disease.

1356 MKK4 Activation Inhibits Metastatic Colonization of the Lung

TL Lotan, DJ Vander Griend, M Kocherginsky, K Macleod, CW Rinker-Schaeffer. University of Chicago, Chicago, IL; Johns Hopkins University, Baltimore, MD.

Background: MAP Kinase Kinase 4 (MKK4) is a metastasis suppressor protein implicated in the regulation of metastasis formation in prostate, ovarian, pancreatic and breast cancers. Originally described in the Dunning AT6.1 prostate cancer model, ectopic expression of MKK4 protein leads to a dramatic (90%) decrease in macroscopic lung metastases. We used this model to study the effects of MKK4 activity on specific steps in spontaneous metastasis.

Design: AT6.1 rat prostate carcinoma cells stably expressing MKK4 protein or vector were injected subcutaneously into more than 40 male SCID mice. Lungs and primary tumors were harvested at 22 or 35 days post injection (dpi). The number of disseminated cells in each lung was determined by a novel quantitative real-time PCR (q-RTPCR) assay. MKK4 activity was assessed by in vitro kinase assay and in situ immunolabeling for phospho-JNK (p-JNK). The biological outcome of MKK4 activation in early metastases was studied by immunolabeling for markers of proliferation (Ki-67, pH3 and BrdU) and apoptosis (cCaspase 3, TUNEL) with computer-aided image analysis.

Results: At 22 dpi, rare micrometastases were visible in the lungs of AT6.1-vector and AT6.1-MKK4 tumor bearers. On the order of 10^4 disseminated cells were detected in both groups with q-RTPCR. By kinase assays, ectopic MKK4 was active in the disseminated cells, but not in the primary tumors expressing MKK4. At 35 dpi, overt metastases were seen in control animals, while animals with MKK4-expressing tumors showed predominantly micrometastatic disease. p-JNK staining was positive along the interface of metastasis and lung tissue. Few apoptotic cells were detected in the MKK4-micrometastases, however the proportion of Ki-67-positive cells was significantly lower in this group compared to control metastases after correction for size ($p<0.0001$, mixed effects model analysis of variance).

Conclusions: This study demonstrates that similar numbers of cells initially disseminate to the lung from both control and MKK4-expressing primary tumors and that ectopic MKK4 shows context-dependent activation within these cells. This activity results in decreased proliferation of disseminated cells, without detectable effect on apoptotic activity. More detailed studies of cell cycle markers will help to elucidate the precise mechanism by which MKK4 inhibits metastatic colonization.

1357 Expression and Localization of C-MET Tyrosine Kinase in Solid Tumors

AC Mackinnon, Jr, M Tretiakova, J Manaligod, R Salgia, T Krausz, AN Husain. University of Chicago, Chicago, IL.

Background: C-MET is a receptor tyrosine kinase that is normally expressed in the epithelium of a wide range of human tissues. Upon binding its ligand, hepatocyte growth factor (HGF), C-MET signaling mediates a host of cellular responses including cell proliferation, motility, invasion, metastasis, and angiogenesis. Furthermore, C-MET activity has been shown to be dysregulated in solid tumors. Because C-MET overexpression is associated with a more aggressive growth pattern and a worse prognosis in carcinoma, C-MET is an excellent pharmaceutical target for the treatment of cancer. The goal of this project is to characterize both the expression levels and subcellular localization of C-MET in five different solid tumors: lung, ovarian, breast, colonic, and renal carcinomas.

Design: We examined C-MET expression in archival, paraffin-embedded lung (n=36), colon (n=38), ovary (n=40), breast (n=35), and renal (n=40) carcinoma specimens by immunohistochemistry. Expression and subcellular localization of C-MET and activated C-MET (Y1003-PO_4) were analyzed.

Results: 70% of ovarian, 77% of breast, 81% of lung, 88% of renal, and 100% of colonic carcinomas showed C-MET expression. Compared to matched, normal, non-neoplastic control tissue, C-MET was dramatically overexpressed in all of the carcinoma specimens. Interestingly, the subcellular localization of C-MET was tissue specific. Expression was restricted to the cytoplasm in 89% of breast carcinoma. In contrast, C-MET was localized to both the membrane and cytoplasm in 68% of ovarian, 76% of lung, 86% of renal, and 89% of colonic carcinomas. Only 3% of lung and renal carcinomas showed exclusive membrane localization. Significantly greater levels of activated C-MET(Y1003-PO_4) with extensive nuclear localization was observed in lung carcinoma compared to the other solid tumor specimens.

Conclusions: C-MET is overexpressed in the majority of all types of solid tumors that we examined. The subcellular localization of C-MET was tissue specific with most C-MET localized to the cytoplasm in breast carcinoma versus both cytoplasmic and membrane localization in lung, ovarian, colonic, and renal carcinomas. In addition, lung carcinomas showed an increase in both the total level and the nuclear localization of activated C-MET(Y1003-PO_4) compared to the other tumor specimens. These findings suggests that C-MET activity during oncogenesis may vary depending upon the cellular context.

1358 Reduced p63 Expression and Elevated Apoptosis in Focally Disrupted Basal Cell Layers: Implications for Prostate Tumor Invasion

YG Man, XL Chen, FU Garcia, WA Gardner. Armed Forces Institute of Pathology and American Registry of Pathology, Washington, DC; Drexel University Colleage of Medicine, Philadelphia, PA.

Background: In normal and pre-invasive prostate tumors, the epithelium is physically separated from the stroma by the basement membrane and basal cell layer, whose disruption is pre-requisite for tumor invasion. Our previous studies suggested that basal cell layer disruptions were triggered by a localized degeneration of aged or injured basal cells and leukocyte infiltration (Man and Sang. Exp Cell Res 301: 103-118; 2004; Man et al. Cancer Detect Prev 29: 161-169, 2005). This study attempted to further identify early signs and unique molecules associated with basal cell degeneration.

Design: Consecutive sections were made from pre-invasive prostate lesions containing ducts and acini with (n=20) and without (n=20) focally disrupted basal cell layers. The expression of different tumor suppressors and apoptotic index in basal cells of different ducts and acini with and without focal basal layer disruptions, and in basal cells of the same duct near and distant from a disruption were assessed, using double immunohistochemistry and an apoptosis detection kit.

Results: Basal cells within focally disrupted basal cell layers or near a given focal disruption showed a significantly lower expression of p63 and higher index of apoptosis, compared to their counterparts in ducts with an intact basal cell layer or distant from a given disruption. A vast majority of the apoptotic basal cells and basal cells without p63 expression were located near focal disruptions, and were often surrounded by or adjacent to immunoreactive cells. Tumor cells overlying focally disrupted basal cell layers often showed increased proliferation, along with distinct alterations in cell density and polarity.

Conclusions: Reduced p63 expression and elevated apoptosis are likely to represent risk factors for basal cell degeneration and might have clinical value in predicting prostate tumor invasion. Supported by grants DAMD17-01-1-0129, DAMD17-01-1-0130, PC051308 from Congressionally Directed Medical Research Programs, and 05AA from AFIP/ARP Initiative fund to Dr. Yan-gao Man

1359 The Use of Pooled Reference RNA in Leu of Matched Normal Cells Results in Significant Discrepancies When Compared to Neoplastic Cells on an Expression Array

WD Mojica, LA Hawthorn, A Arshad. University at Buffalo; Roswell Park Cancer Institute, Buffalo, NY.

Background: Messenger RNA expression analysis can result in a tremendous amount of data. In the comparison between two samples, a differentiated/normal cell should be contrasted to a de-differentiated/tumor cell, preferably of the same lineage. The virtual absence of normal cells available for molecular studies precludes their incorporation into most studies. As a result, pooled reference RNA has been suggested as an alternative standard. It is currently unknown what similarities or differences exist when pooled reference RNA is used instead of normal cells and compared to matched dedifferentiated/neoplastic cells in a microarray expression study.

Design: Matched normal and neoplastic cells were separately procured from a surgical hemicolectomy specimen by manual exfoliation followed by enrichment with immunomagnetic beads (Dynal Epithelial Enrich, Invitrogen, Brown Deer, WI). RNA was isolated using a commercially available phenol+guanidine isothiocyanate solution (Trizol, Invitrogen, Carlsbad, CA) followed by purification on spin columns (Qiagen Min Elute, Qiagen, Valencia, CA). Sufficient RNA was retrieved from the clinical samples negating the need for amplification. RNA from enriched normal colonic epithelial cells, neoplastic colonic epithelial cells and reference pooled cell lines (Universal Human Reference RNA, Stratagene, La Jolla, CA) were hybridized unto separate Affymetrix HGU133 Plus 2.0 chips. Data sets between matched normal + tumor cells were compared to results from pooled reference RNA + tumor cells using GeneTraffic microarray analysis software (Iobion, Stratagene, La Jolla, CA).

Results: There were 679 common 2 fold increases and 45 common 2 fold decreases when analysis was performed between data from matched normal + neoplastic cells and compared to pooled reference + neoplastic cells. There were 5808 discrepant results when these two groups were analyzed (e.g., a 2 fold or greater increase observed in a given gene in the comparison of normal to neoplastic with no or decreased expression in the same gene in the comparison of pooled reference to neoplastic cells).

Conclusions: The expression of genes in pooled reference RNA are different from normal colonic epithelial cells. Pooled RNA from cell lines may be suitable as a reference source, but caution should be taken when interpreting data involving its incorporation in studies with neoplastic cells from clinical specimens.

1360 CDX-2 Immunostaining in Pseudomyxoma Peritonei

D Nonaka, S Kusamura, D Baratti, P Casali, R Younan, M Deraco. New York University Medical Center, New York, NY; National Cancer Institute, Milan, Italy.

Background: The immunohistochemistry of transcription factors, due to their high specificity, have become immensely important in the field of diagnostic pathology. Examples include TTF-1, myogenin, MITF and CDX-2. Among them, CDX-2 is a highly sensitive and specific marker of intestinal epithelial cells and their neoplastic counterparts. Pseudomyxoma peritonei (PMP) is a condition characterized by the accumulation of abundant gelatinous mucin materials within the peritoneal cavity, with the neoplastic epithelial component being particularly sparse. Currently, an appendiceal origin is favored on immunohistochemical and molecular grounds. CDX-2 status in PMP has been scarcely reported in the literature. We report on clinicopathologic features of 42 cases of PMP with a special emphasis on CDX-2, along with a panel of other immunohistochemistry markers.

Design: All 42 patients were treated at a single institution uniformly by means of cytoreduction surgery. Immunohistochemical stains were performed for CDX-2, MUC-2, MUC-5AC, CK7 and CK20. Statistic correlation was also evaluated for age, sex,

completeness of cytoreduction (CC), and histologic subtype with overall and progression free survivals (OS and PFS).
Results: There were 26 males and 16 females, with ages ranging from 24 to 76 (median, 53 years). PMP consisted of 32 cases of disseminated peritoneal adenomucinosis (DPAM) and 10 cases of peritoneal mucinous carcinomatosis (PMCA). The appendix was also evaluated in 25 cases (60%), showing mucinous neoplasms in 23 cases (92%); 2 mucinous adenocarcinomas (MACAs), and 21 low-grade appendiceal mucinous neoplasms (LAMNs). CDX-2 was diffusely positive in 40 cases (95%), with the remaining 2 cases being focally positive. As expected, CK20 was diffusely positive in all the cases, CK7 was variably positive in 38 cases, MUC-2 positive in all 42 cases and MUC-5AC variably positive in all 42 cases. All patients were optimally cytoreduced. 5-year overall survival was 97%. Histologic classification was significantly correlated with PFS (p=0.02).
Conclusions: CDX-2 is diffusely and strongly positive in PMP. This is a useful marker to confirm an appendiceal origin of PMP, particularly when used in conjunction with CK7, CK20, MUC-2 and MUC-5AC. Given that PMCA was correlated with a worse outcome than DPAM, it is therefore recommended that PMP be pathologically classified into these two groups.

1361 Oligonucleotide and Immunohistochemical Analysis of Claudin-7 in Normal Human Epithelia and Their Malignant Counterpart

HS Qureshi, G Hampton, W El-Rifai, HF Frierson. University of Virginia, Charlottesville, VA; Genomics Institute of the Novartis Research Foundation, San Diego, CA.
Background: Claudins are transmembrane proteins which are contained in tight junctions and are connected to the actin cytoskeleton by ZO-1. This is the first study which explors the prescence of Claudin-7 in normal human tissue and carcinomas of various sites.
Design: Claudin-7 expression was analysed in Oligonucleotide microarrays that we used previously for 168 carcinomas of various sites. The level of expression was determined by hybridization to U95a GeneChips (Affymetrix, Santa Clara, CA). Relative Flourescence Units were used to divide the tumors into 4 groups: Low (<300), moderate (300-999), high (1000-1999), and very High (>2000). Further, Immunohistochemistry using an antibody to Claudin-7 (goat polyclonal, Santa Cruz, CA) was performed on 127 normal human epithelia and 164 carcinomas of various sites. The immunostain was considered positive when at least partial membrane staining in > 10 % of the cells was present.
Results: Please see table 1.
Conclusions: Claudin-7 expression by immunohistochemistry was present in normal colorectal, endometrium and pancreatico-biliary carcinomas, while abscent in ovary, breast, lung, liver, thyroid, kidney, stomach, prostate and urinary bladder. An increase in gene/protein over expression compare to normal was found in carcinomas of ovary, breast, endometrium, lung, thyroid, stomach, prostate and urinary bladder. While no difference was found in Colorectal and renal carcinomas. In Pancreatico-biliary carcinomas the Claudin-7 expression was reduced compared to normal tissue. Claudin-7 may play a critical role in tumor progression and biology. The mechanism of Claudin-7 overexpression in various carcinomas remains to be explored.

Claudin-7 expression in normal human epithelia and their malignant counterparts by Immunohistochemistry and Oligonucleotid microarrays

Site	Normal IHC % positive	Tumor IHC % positive	Tumor mRNA Range RFU	Tumor mRNA Mean RFU
Colon	77	73	455-3338	1360
Ovary	0	45	323-1735	781
Breast	0	25	123-1205	564
Endometrium	43	70	not done	not done
Lung	0	28	74-2542	753
Pancreatic-biliary	88	50	319-1311	654
Liver	0	0	147-930	417
Thyroid	0	100	not done	not done
Kidney	0	8	63-394	164
Stomach	0	35	41-5700	1973
Prostate	0	62	-8-1709	658
Urinary Bladder	0	not done	352-1659	841

IHC=Immunohistochemistry, RFU= Relative flourescent Units

1362 In Search of a "Joker" Factor in Cell Signaling Pathway in Human Malignant Tumors. 4EBP1 as a Very Good Candidate

S Ramon y Cajal, J Jimenez, E Llonch, F Rojo, M Cuatrecasas, C Iglesias, J Castellvi, A Garcia, J Baselga, H Allende. Vall d'Hebron University Hospital, Barcelona, Spain.
Background: Growth signaling pathways suffer deregulation in all tumors and acquired growth signals autonomy is basic in malignancy. That autonomy may be due to alterations in transcellular transducers or intracellular circuits. Those circuits with a myriad of cellular factors which may interact in an extremely complex biochemical machinery, with major pathways as PI3K/AKT, ras-raf-MAPK or Wnt/catenin. Importantly, most of those pathways should converge in final drivers which transmit the proliferative signal and control protein synthesis
Design: We have analyzed 720 formalin-fixed malignant carcinomas (120 ovary, 103 breast, 133 colon, 55 prostate, 104 endometrial, 180 cervix, 25 gastric) with a immunohistochemical profile including multiple phosphorylated (p) proteins: AKT, 4EBP1, p70S6K and S6 as well as HER2 and EGFR. Levels of expression were evaluated as a score combining percentage and intensity of stained tumor cells (Hscore)
Results: Some of results included are shown in breast, colon, prostate and gynecology sections. The first remark to underline is that detection of activated-proteins using phospho-specific antibodies is feasible in paraffin sections and observed results are consistent and reliable. Concomitantly, western-blot or tissue lysate assays are extremely informative to validate specificity and sensitivity of used antibodies and this scoring method. Of all the markers studied, p4EBP1 is detected up to 73% of tumors, whereas pAKT is detected in only 45% of specimens and MAPK in 51%. Clinically, p4EBP1 is mainly expressed in poor differentiated tumors and correlates with presence of metastases, local recurrence and/or survival
Conclusions: 1. The pathway PI3K/AKT/mTOR is activated in most types of carcinomas with percentages ranging from 42% in breast to 75% in endometrial carcinomas. In our series, pAKT does not discriminate low and high malignant tumors 2. Of all the proteins studied, p4EBP1 is the only factor to be related with histological grade of malignancy, metastases and local recurrence or survival in ovary, breast, colon, endometrial and cervical carcinomas 3. In brief, p4EBP1 can be activated by PI3K/AKT, MAPK, phospholipase D/mTOR, lack of p53 and other kinases not well characterized, can be a "joker" factor which drive the oncogenic signal of the main biochemical pathways involved in cell signaling transduction and p4EBP1 overexpression can reflect an accumulation of multiple upstream genetic alterations

1363 Egr-1 Regulates Hypoxia-Induced Tissue Factor Expression and Plasma Coagulation by Glioblastoma

Y Rong, RP Huang, RL Jensen, DL Durden, EG Van Meir, DJ Brat. Emory University, Atlanta, GA; University of Utah, Salt Lake City, UT.
Background: Pseudopalisading necrosis in glioblastoma (GBM) indicates rapid tumor growth. We suggest that intravascular thrombosis promotes pseudopalisade formation and the ensuing angiogenic cascade. Tissue factor (TF), the main cellular initiator of blood coagulation, is overexpressed in astrocytomas and may contribute to thrombosis. Here we investigated the roles of early growth response-1 (Egr-1) and hypoxia-inducible factor (HIF) in the hypoxic regulation of TF in GBM cells.
Design: We examined the effect of hypoxia (1% O_2) on TF expression and plasma clotting using a clone of the GBM cell line U87MG (23-11). Egr-1, HIF-1α, and TF expression were assessed by IHC, IF, real-time PCR, and Western blot. Plasma clotting times were measured using a tilt-tube assay. siRNA directed at *Egr-1* and *HIF-1α* were used for selective knock down, while expression plasmids were used to increase cellular levels. Gel shifting experiments and luciferase reporter constructs we used to investigate hypoxia-induced binding of transcription factors and transcriptional activity, respectively.
Results: Hypoxic 23-11 glioma cells induced plasma clotting at 65 ± 2 sec, significantly shorter than normoxic cells (21% O_2; 136 ± 4 sec). Both antibodies directed at TF and plasma lacking Factor VII greatly inhibited hypoxia-induced clotting. Marked increases in TF mRNA and protein were noted in 23-11 cells after 6 hrs of hypoxia and peaked after 24 hrs. Hypoxia also caused increased Egr-1 mRNA and protein expression within 1h, preceding the upregulation of TF. Overexpression of Egr-1 following cDNA transfection caused upregulation of TF under normoxia, whereas siRNA directed at *Egr-1* attenuated hypoxia-induced TF expression. We detected enhanced nuclear localization of Egr-1 under hypoxia by IF and gel shifting studies showed hypoxia-induced binding of Egr-1 to the *TF* promoter sequence. Egr-1 dependent transcriptional activity detected with a luciferase reporter increased significantly under hypoxia as compared to normoxia or serum stimulation. *HIF-1α* mRNA silencing did not affect TF expression under hypoxia while it significantly inhibited both HIF-1α and VEGF expression.
Conclusions: Hypoxia causes increased TF expression and accelerated plasma clotting by GBM cells. Hypoxic upregulation of TF depends on Egr-1 and is largely independent of HIF-1α. These factors could contribute to TF dependent intravascular thrombosis and necrosis in GBM.

1364 Expression of the Novel Gene RSK4 in Human Tumors: A mRNA Study

C Ruiz-Marcellan, L Lopez, M Lleonart, J Castellvi, A Garcia, V Fumanal, J Hernandez, I de Torres, F Rojo, A Lopez, S Ramon y Cajal. Vall Hebron University Hospital, Barcelona, Spain; Hospital S Pere de Ribes, Barcelona, Spain.
Background: Ras-dependent mitogen activated protein MAP kinase cascade regulates cellular division, survival and differentiation via phosphorylation of numerous intracellular proteins. RSK4 has been proposed as an inhibitor of this pathway and as well, to mediate p53-induced growth arrest. The aim of this work is to study the mRNA level of RSK4 in colon, prostate, lung, kidney carcinomas and in gliomas and lymphomas in order to correlate it with clinic-pathological characteristics.
Design: 30 lymphomas, 7 renal cell carcinomas, 11 gliomas, 20 colon carcinomas, 20 lung carcinomas and 20 prostate carcinomas were analyzed. RNA was extracted from both normal and tumor tissues of each patient. The real-time PCR was performed using Taqman probes corresponding to RSK4 and p53 genes (ABI PRISM 700 SDS). As an endogenous control gene, ciclofilin was amplified. Positive controls for each gene were also included. Tonsils and white blood cells were used as control for the lymphomas.
Results: In colon and renal cell carcinomas and in gliomas, RSK4 was highly downregulated respect their respective controls. In 50% lung carcinomas, RSK4 was also downregulated and in prostate carcinomas there were not significant differences. In lymphomas, there was a striking upregulation of RSK4 in 4 out 10 large cell B lymphomas.
Conclusions: MAPK pathway is related to cell proliferation or differentiation according the cell type.The downregulation of RSK4, as an inhibitor of this pathway, may then induce cell proliferation in colon, brain and renal tumors supporting an important role of this pathway in these tumors. In a set of lymphomas, upregulation of RSK4, may be associated with lack of diffentiation via the inhibition of MAPK. Further studies are needed to evaluate the real role of RSK4/MAPK in lymphomas and in a specific set of carcinomas.

1365 Galectin-4 Expression in Carcinoid Tumors

K Rumilla, LA Erickson, AK Erickson, RV Lloyd. Mayo Clinic, Rochester, MN; South Dakota State University, Brookings, SD.

Background: Galectins (Gal) are an evolutionary conserved family of 15 lectin-binding proteins which are widely distributed in normal and neoplastic cells. They have roles in inflammatory reactions, cell adhesion, tumor progression and metastasis. The function and distribution of Gal-3 and Gal-1 are well characterized but little information is known about Gal-4. Recent studies have localized Gal-4 in the enterochromaffin cells of the small intestine.

Design: We examined tissue microarrays of 44 primary and 52 metastatic ileal carcinoids by immunohistochemistry with monoclonal antibodies to Gal-4, Gal-3 and Gal-1. Pulmonary (n=7), rectal (n=6), and gastric (n=6) carcinoids were also examined with larger tissue sections. Western blotting of 3 ileal carcinoids was also done using all three antibodies.

Results: Gal-4 was most highly expressed in ileal carcinoids. Western blotting showed a 32kDa band for Gal-4 in the 3 ileal carcinoids. Gal-3 and Gal-1 were not detected in ileal carcinoids by Western blotting. Gastric carcinoids also expressed Gal-4, but very few pulmonary or rectal carcinoids were positive for Gal-4 (p=0.002). There was decreased expression of Gal-4 in metastatic compared to primary ileal carcinoids (p=0.069). Much lower levels of Gal-1 and Gal-3 were present in ileal carcinoids compared to pulmonary and rectal tumors by immunohistochemistry.

Conclusions: These results show a differential distribution of Gal-4, Gal-3 and Gal-1 in ileal carcinoids compared to lung and rectal carcinoids. The lower levels of expression of Gal-4 in metastatic ileal carcinoids compared to primary tumors may contribute to decreased cell adhesion and metastasis in these carcinoid tumors.

1366 The Role of Regulatory T-Cells in Immunologically Preparing Secrertory Endometrium for Fetal Implantation

HA Sattar, AN Husain, X Fu, A Montag, M Tretiakova, T Krausz. University of Chicago Hospitals, Chicago, IL.

Background: Implantation of the fetus into the maternal endometrium and uterine wall is an important event in pregnancy. This invasion of fetal cells into the environment of maternal immunity requires local down-regulation of the maternal cellular immune response. Recently, interest has been rekindled in a specialized subset of CD4+ T-cells known as T-regulatory cells. These cells express CD25 and Foxp3, and have been shown to play a role in the establishment of localized immunotolerance. More specifically, it has been shown that CD4+CD25+ regulatory T-cells are present in decidua of early pregnancy and spontaneous abortion. Given that lymphocytes accumulate in the endometrium as it cycles through early, mid, and late secretory phases, we postulated that some of this lymphocytic increase might be due to the accumulation of specialized regulatory T-cells, in effect preparing the endometrium for implantation of the fetal graft.

Design: Ten cases of proliferative endometrium and ten cases each of early, mid, and late secretory endometrium were gathered from our pathology archives. The specimens consisted of diagnostic biopsies taken over a one-year period (2004-2005). Each case was immunostained for CD3, CD4, CD8, CD20, CD56, CD25, and Foxp3.

Results: Progression of endometrial samples along the secretory cycle revealed a definite increase in CD3+ T-lymphocytes, predominantly of the CD56+ NK cell lineage, with no significant change in the numbers of CD4, CD8, and CD20 positive cells. A significant number of T-regulatory cells was not appreciated. In fact, the lymphocytes present in samples from all stages of endometrial cycling showed virtually complete lack of CD25 or Foxp3 immunoreactivity.

Conclusions: Lymphocytes increase during the secretory phase of the endometrial cycle. However, this is not accompanied by a significant number of CD4+CD25+Foxp3+ regulatory T-cells. Although regulatory T-cells may play a role in immunosupression at the maternal-fetal interface, these cells do not accumulate as the endometrium cycles through secretory phase. Hence, regulatory T-cells are not involved in immunologically preparing the endometrium to receive the fetal graft. Further studies to determine the presence of T-regulatory cells at the implantation site are currently in progress.

1367 The Role of α2β1 Integrin in Tumor Angiogenesis and Stromal Organization in the K14-HPV16 Transgenic Mouse Model of Squamous Cell Carcinoma

AM Sheehan, LE Wells, MM Zutter, LM Coussens. Vanderbilt University Medical Center, Nashville, TN; University of California, San Francisco, San Francisco, CA.

Background: The α2β1 integrin, a cell surface receptor for collagens and laminins, is expressed on a variety of cell types including epithelial cells. Expression is enhanced in proliferating epithelium, such as basal cells of stratified squamous epithelium, suggesting that α2β1 integrin is associated with orderly cell proliferation. Our lab described generation of a genetically engineered α2β1-null mouse. Transgenic mice expressing HPV16 early region genes under direction of the K14 promoter have been described and used as a model for squamous carcinogenesis. To define potential roles of α2β1 integrin in carcinogenesis, epithelial-stromal interactions, and angiogenesis, we have generated wild type and α2β1-null mice expressing the K14-HPV16 transgene.

Design: K14-HPV16 transgenic mice were crossed with α2β1 integrin-null mice to generate transgenic K14-HPV16 animals with either wild type or α2β1-null genotype. Wild type (8 mice) and α2- null (9 mice) K14-HPV16 mice were followed for 6 months. Biopsies of ear and trunk skin were obtained at 3 and 6 months, formalin-fixed, paraffin-embedded, and stained with H&E. 6 month biopsies were stained with trichrome, and immunohistochemistry performed for CD31. Sections were evaluated morphologically, and quantitative studies of blood vessel number and area were performed using image analysis software (Metamorph, Molecular Devices Corporation, Sunnyvale, CA)

Results: At age 6 months, epithelial changes were similar in wild type and α2β1-null mice. All animals demonstrated significant epithelial hyperplasia with mild to moderate dysplasia and parakeratosis but without invasion. In contrast to the epithelial similarities, there were stromal differences. Both blood vessel number and area were increased in trunk skin of K14-HPV16 α2β1-null mice compared to wild-type. In addition, morphology of H&E and trichrome stained sections suggested increased density of collagen fibers in trunk skin of K14-HPV16 α2β1-null mice versus wild-type.

Conclusions: Our findings show increased blood vessel number and area, as well as increased density of collagen fibers in K14-HPV16 α2β1-null mice versus wild type controls. These findings suggest the integrin modulates host stromal response in a model of HPV associated squamous carcinoma. Examination of these mice at later time points for invasion and metastasis should shed further light on the role of α2β1 integrin in tumor-stromal interactions.

1368 Precancer Stem Cells Are Potentially a Common Progenitor of Various Tumor Components

R Shen, L Chen, J-X Gao. Ohio State University, Columbus, OH.

Background: A solid tumor is composed of cancer cells, blood vessels, and supporting stromas, which determine its growth rate and malignancy. However, the origin of various components of the tumor is largely unknown, hampering the development of efficient strategy for tumor therapy. Cancer stem cells (CSCs), in which normal developmental program is not completely abolished, have recently been identified as a progenitor of cancer cells, implicating that many tumor components may share a common progenitor with CSCs. Recently, we have established three clones of precancer stem cells (pCSCs) from the spleen of a $p53^{-/-}$Stat-$1^{-/-}$ mouse with lymphoma, which not only can differentiate into various normal tissue-committed cells, but also into various types of cancer cells, depending on environmental cues of the recipients. Based on these observations, we hypothesized that pCSCs can be a common progenitor of cancer cells, blood vessels, and stromal tissues in solid tumor.

Design: To test the hypothesis, we develop a pCSC line stably expressing enhanced green fluorescent proteins (eGFPs) by transducing a pCSC clone 2C4 with eGFP lentiviral vectors. The pCSCs or $eGFP^+$ pCSCs were injected i.p. or s.c. into the severe combined immunodeficient (SCID) mice to induce solid tumors. The origin of tumor components including cancer cells, blood vessels, and stromal tissues was systematically analyzed by flow cytometry and/or immunohistochemistry. In addition to eGFP, the pCSC-derived tumor components were identified also by antibody to neomycin, which is a product of neomycin gene integrated to genome DNA of pCSCs.

Results: The pCSCs developed solid tumor in 40 ~ 70% recipients, depending on experiments. More than 95% tumor cells were derived from $eGFP^+$ pCSCs as revealed by flow cytometry. Among them about 5 ~ 10% cells were Lin^+ with the eGFP being hierarchically down regulated; and about 40 ~ 80% of Lin^+ cells were $CD45^-$. Pathological analysis demonstrated that in addition to cancer cells, pCSCs can also develop into skeletal muscles, blood vessels and adipose tissue. Different developmental stages of skeletal muscles and blood vessels were observed in the tumor tissue. Immunohistochemical stains confirmed that the skeletal muscles and blood vessels, like cancer cells, were derived from pCSCs.

Conclusions: Our results for the first time reveal that tumor components can be derived from a common progenitor such as pCSCs. Therefore, pCSCs can be used as a novel target for anti-cancer drug development, cancer prevention, and immunotherapy.

1369 A Knock-In Mouse Model of Gastrointestinal Stromal Tumor Harboring *kit* K641E: Utility as a Pre-Clinical Model

MR Tanas, ML Comstock, RS Miyaoka, J Woodell, BP Rubin. University of Washington, Seattle, WA.

Background: A mouse model of gastrointestinal stromal tumors (GIST) has been developed by knocking in a *kit* gene K641E mutation, originally identified in sporadic human GISTs and as a germ line mutation in familial GIST syndrome patients, into the mouse genome. The K641E phenotype includes ICC hyperplasia and cecal GISTs, which are morphologically and immunohistochemically identical to human GISTs. Imatinib mesylate (known comercially as Gleevec, Novartis Pharmaceuticals, Basel, Switzerland), a small molecule inhibitor of kit receptor tyrosine kinsase, has been shown to be useful in treating patients with metastatic GISTs. Positron emission tomography (PET) imaging has been used clinically to assess response of GISTs to imatinib therapy; reduced uptake of [F-18]- fluorodeoxyglucose (FDG) is considered to correlate with a favorable response to therapy. With the advent of imatinib resistance, mouse models may offer an economical and efficient way to evaluate new anti-kit/anti-GIST therapies.

Design: *Kit* K641E mice are imaged by PET scan with FDG prior to treatment with imatinib mesylate. Imatinib (100mg/kg/qd) is administered over a 3 day period by oral gavage, with a follow-up PET scan taken to determine the metabolic activity of these tumors after treatment. The metabolic activity of GISTs as measured by PET is correlated with kit phosphorylation status, measured in both non-treated control tumors and treated tumors by western blot analysis using antibodies to kit and phosphokit (Cell Signaling Technology, Beverly, MA).

Results: PET scans of *kit* K641E mice before and after treatment with imatinib demonstrated a decrease in their metabolic activity. This corrleated with western blot results, which showed a concurrent decrease in the level of kit tyrosine phophorylation in treated GISTs.

Conclusions: GISTs in *kit* K641E mice respond to treatment with imatinib mesylate both by PET imaging and at the biochemical level as measured by a decrease in kit receptor tyrosine kinase phosphorylation, as is seen in human GISTs. Therefore, this model should be very useful in the preclinical evaluation of new anti-kit/anti-GIST therapies that will be developed for the treatment of human GISTs.

1370 Global Expression Profiling of Microdissected Tumor Associated Vasculature

BD Tarlow, LA Strickland, Z Modrusan, TD Wu, HW Koeppen. Genentech, Inc, South San Francisco, CA.

Background: Endothelium that lines the vasculature in tumors has been demonstrated to be qualitatively different from endothelium in normal blood vessels. Gene expression changes in tumor endothelium have been difficult to study because these cells comprise only a small fraction of all cells in a heterogeneous tissue. Moreover, tumor vasculature engages in complex microenvironment signaling with stroma and epithelium that is difficult to simulate in vitro. Here, we enriched endothelial cells from human colon cancer tissues with laser capture microdissection and examined global differential gene expression in tumor vasculature.

Design: Vasculature in normal and malignant human colons was identified in situ by immunofluourescent labeling with a monoclonal α-CD146 antibody conjugated to Alexafluor-488 (Chemicon). Immunofluorescently-labeled vascular channels were microdissected with the SL-CellCut laser capture system (Molecular Machines Inc.). RNA was amplified with two rounds of T7-based amplification. Cy5-labeled, amplified RNA was hybridized to the Agilent whole genome microarrays and microarray data was analyzed with Automated Microarray Analysis (Genentech). Enrichment for endothelial cells was validated in the datasets using known endothelial markers. Contamination of the samples was assessed using known markers for epithelial cell and smooth muscle.

Results: Microdissected tissue showed enrichment of known endothelial markers CD34, CD31, von Willebrand factor, and vascular endothelial growth factor receptor-2 (VEGFR-2) in both normal and tumor microdissected samples ($p<0.01$). We identified genes showing strong expression in tumor vasculature relative to normal vasculature and undissected tissue. Our data set confirms preferential tumor endothelial expression of VEGFR-2, angiopoietin-2, and CD34. Additionally, we will report preferential tumor endothelial expression of several novel sequences previously uncharacterized in tumor endothelium.

Conclusions: Laser microdissection is a powerful tool for the enrichment of endothelial cells and the identification of novel molecules preferentially expressed in tumor vasculature. This study has identified several novel sequences, including putative transmembrane molecules as potential tumor angiogenesis biomakers. Tumor endothelial specific molecules may serve as targets for anti-angiogenic therapies. Studies to evaluate the expression pattern of these novel molecules in situ are ongoing and will permit the validation of our dataset.

1371 Transcriptional Regulation of Valosin-Containing Protein (VCP) Gene, Which Is Involved in Cell Proliferation and Metastasis, through PBX1 (Pre B Cell Leukemia Transcription Factor 1)

Y Tomita, Y Qiu, Z Zhang, I Nakamichi, E Morii, K Aozasa. Osaka University Graduate School of Medicine, Suita, Osaka, Japan; Medical School of Tongji University, Shanghai, China.

Background: Valosin-containing protein (VCP) is involved in a wide variety of cellular functions. Previous study showed that the enhanced expression of VCP in cancer cells correlates with invasion and metastasis of cancers.

Design: The present study was employed to investigate the regulation mechanism for VCP transcription.

Results: A Luciferase reporter assay with plasmids containing serially deleted 5´-flanking region of VCP and MCF7 cells revealed a decrease in reporter activity when the promoter region between -115 and -112 was deleted. Pre B-cell leukemia binding factor 1 (PBX1) binding motif was found between -110 and -113, thus this region was considered to be essential for VCP transcription. Additional three PBX1 binding sequences at -181, -295, and -694 were found in the 5´-flanking region of VCP.

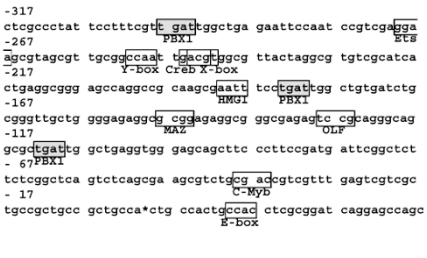

Introduction of mutation/deletion in the PBX1 binding motifs resulted in 93-97% decrease in reporter activities compared to the wild constructs.

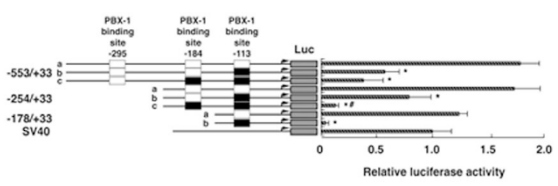

Co-transfection of PBX1-expression plasmid increased the reporter activities of constructs containing PBX1 binding motifs by 1.45-1.87 times. Whereas little change was observed with the construct devoid of PBX1 binding sites. Binding of PBX1 to the 5[acute-flanking sequence of VCP was shown by chromatin immunoprecipitation assay.

Conclusions: These findings indicate that PBX1 is an important transcription factor for VCP expression.

1372 Loss of CBX7 Expression Is a Common Event in Human Malignancies

G Troncone, P Pallante, M Sanchez-Beato, MT Berlingieri, A Iaccarino, M Russo, L Palombini, A Fusco. Università degli Studi di Napoli Federico II, Naples, Italy; Centro Nacional de Investigaciones Oncologicas, Madrid, Spain; NOGEC (Naples Oncogenomic Center)-CEINGE, Biotecnologie Avanzate, Naples, Italy.

Background: CBX7 is a novel Polycomb group protein (PcG) acting as a repressor of gene transcription. This gene was identified by the analysis of a microarray gene profile of several thyroid carcinoma cell lines versus normal thyroid cells. Since CBX7 expression was drastically downregulated in thyroid carcinoma cell lines, the loss of this protein may be related to the malignant phenotype. To evaluate wheter loss of CBX7 is a common event in human malignancies this study was undertaken to screen its expression in normal and neoplastic tissues.

Design: A multi-tumour tissue microarray constructed using 484 tumours (for each sample two duplicate) of 56 (10 benign and 46 malignant) different types and a normal-tissue microarray constructed using 310 sample from 42 different tissues were stained for CBX7 by an antibody raised against CBX7 specific peptide (recombinat protein). The results were further confirmed in selected tumour types (thyroid, ovary and breast) by RT-PCR.

Results: CBX7 expression was always observed in all the different samples of the normal-tissue microarray. Benign tumours also maintained CBX7 expression, with the only exception of 30% of dysplastic colonic adenomas. Eighty nine % (41/46) of the malignant tumour types examined showed a variable degree of CBX7 loss of expression. The tumours showing the higher rate of CBX7 loss of expression (>75% of negative neoplastic cells) were follicular thyroid carcinoma, Hodgkin lymphoma, germ cell carcinoma of the testis and lung carcinoma. This results were confirmed by RT-PCR.

Conclusions: CBX7 pattern of expression in normal and in neoplastic tissue suggests that this protein could act as a putative onco-suppressor.

1373 Overexpression of Wild-Type p53 Induced Phosphatase (Wip1) Abrogates p38 MAPK-p53-Wip1 Pathway, Contributing to the Tumorigenesis of Human Breast Cancers

E Yu, Y Ahn, HS Yoon, G Gong, J Choi. University of Ulsan College of Medicine Asna Medical Center, Seoul, Korea.

Background: The wild-type p53 induced phosphatase (Wip1, or PPM1D) is a serine/threonine phosphatase that is expressed upon various stresses and selectively inactivates p38 MAPK through dephosphorylation at threonine 180 *in vitro.* Wip1 gene amplification is known in a few human cancers, however, the potential role of Wip1 gene is not defined yet. Especially in breast cancers, previous studies showed that Wip1 might be a driver oncogene at the frequent gain of 17q21-24.

Design: In this study, we examined the expression of Wip1 gene in the level of mRNA and the protein in 20 cases of human breast cancer tissues and 5 breast cancer cell lines. We also investigated the relationship between the expressions of Wip1 and its regulatory proteins including active p38 MAPK, p53 as well as p16 proteins.

Results: Wip1 expression was significantly increased in 7 (35%) of 20 cases of breast cancer tissues and 2 (40%) of 5 cell lines. The Wip1 overexpression was inversely correlated with that of active (phosphor-) p38 MAPK ($p = 0.007$). Furthermore, the Wip1-overexpressed tumors exhibited absent or weak expression of p16 that normally accumulates in accordance with the activation of p38 MAPK ($p = 0.054$). The loss of p16 expression was not associated with hypermethylation of *p16* promoter or loss of heterozygosity on 9p21. All tumors with Wip1 overexpression exhibited a lack of p53 expression, indicating the tumors are wild-type for p53.

Conclusions: These results imply that the Wip1 overexpression abrogates the homeostatic balance that is maintained through the p38-p53-Wip1 pathway, and contributes to the malignant progression by inactivating wild-type p53 and p38 MAPK and decreasing the expression of p16 protein in human breast tissues.

1374 Decreased Fucose Expression Alters the Interaction of Human Breast Cancer Cells with Matrices and Endothelium In Vitro

K Yuan, G Rezonzew, D Kucik, GP Siegal. UAB, Birmingham, AL; VAMC, Birmingham, AL.

Background: Glycosylation plays important roles in cell-cell and cell-matrix interactions. Fucose, a monosaccharide of glycosylation, is over-expressed in many malignant tumors. Using alpha-L-fucosidase, a glycosidase that specifically removes alpha-L-fucose [a-L-f], we studied the potential effects of defucosylation on tumor functions, focusing on tumor progression. Previously, we found a-L-fase pretreatment significantly decreased the invasion of MDA-MB-231 cells and its inhibitor deoxyfuconojirimycin reversed this effect. Fucosidase treatment was also found to inhibit the gelatinolytic activity of matrix metalloproteinase 9 but not MMP-2.

Design: Herein, we extend these studies to the effects of defucosylation on the interaction of tumor cells with the extracellular environment.

Results: We report that a-L-fase treatment decreases tumor cell adhesion to fibronectin, laminin, collagen I, hyaluronic acid and the complex biomatrix (HuBiogel). The immunofluorescence colocalization of beta-1 integrin and fucose was found to decrease accordingly. Using a flow chamber system, we found that a-L-fase treatment decreased the rolling of MDA MB 231 cells on human umbilical vein endothelial cells while significantly increasing their flow speed. The rolling of defucosylated tumor cells also displayed impaired rolling on purified matrices including those containing E-selectin. Sialyl Lewis X [sLX], an a-L-f containing tetrasaccharide, which participates in the rolling of leukocytes and tumor cells on endothelium, was found to be abundantly expressed on MDA MB 231 cells and diminished after a-L-fase treatment. Exogenous sLX significantly interfered with the rolling interaction of tumor cells with endothelium.

Conclusions: Based on these data, we hypothesize that decreased fucosylation impairs the interaction between tumor cells and their external milieu, which in turn, affects key cell functions modulating tumor progression. Decreased adhesion on HUVEC in the presence of fucosidase also evokes the rationale that defucosylation may modulate metastasis, and thus provides a promising approach to hinder tumor progression and dissemination.

1375 Effects of a Monoclonal Anti-αvβ3 Antibody on Blood Vessels – A Pharmacodynamic Study

D Zhang, T Pier, D Alberti, DG McNeel, G Wilding, A Friedl. University of Wisconsin-Madison, Madison, WI.

Background: Angiogenesis is required for wound healing and tumor growth. The integrin αvβ3 is an adhesion molecule expressed by proliferating endothelial cells and antibodies blocking this integrin inhibit angiogenesis in pre-clinical models. Focal adhesion kinase (FAK) is an intracellular signaling molecule, which forms a complex with integrins and growth factor receptors and thus integrates signals generated by both receptor types. MEDI-522 is a second generation humanized monoclonal anti-αvβ3 antibody designed as a therapeutic anti-angiogenic agent. The purpose of this correlative study was to determine the distribution of MEDI-522 in tissues and to examine potential effects on blood vessels.

Design: In a phase I dose escalation study, MEDI-522 was administered by weekly infusions to 25 adult patients with advanced solid organ malignancies. As a surrogate angiogenesis assay, a wound was created by punch biopsy of the arm skin. This wound site was re-biopsied after a 7-day interval. Sequential pre-treatment and four-week treatment biopsy pairs were available on four patients, who had received 6 or 10 mg/kg of MEDI-522. Localization of the therapeutic agent, levels of β3 integrin subunit, vascular density, proliferation and apoptosis of endothelial cells, and phosphorylation state of focal adhesion kinase (p-FAK) were determined by dual-label immunofluorescence and computer-assisted image analysis.

Results: Medi-522 was detected in the perivascular area as well as the dermal interstitium both in intact and wounded skin sites following treatment. No statistically significant difference was found between pre-treatment and treatment samples of skin for vascular density, proliferation and apoptosis of endothelial cells, and αvβ3 integrin levels. However, the immunofluorescence intensity of p-FAK was significantly lower in skin wound vessels during MEDI-522 treatment compared to the pre-treatment samples.

Conclusions: Medi-522 was detectable both in quiescent and in angiogenically active skin blood vessels as well as in the dermal interstitial space. The levels of phosphorylated FAK were reduced during Medi-522 treatment, suggesting a modulating effect on this signaling molecule. Work supported by the National Cancer Institute, UO1 CA62491 and NO2-CO-124001 (22XS082A)

1376 Transgenic Mice Overexpressing Human 8-Oxoguanine DNA Glycosylase (hOGG) in Mitochondria Develop Obesity, Hepatosteatosis and Female Infertility

H Zhang, Q Huang, L Li, Y Wang, MW Zhou, G Ranganathan, PA Kern, PM Iannaccone, CY Fan. University of Arkansas for Medical Sciences, Little Rock, AR; City of Hope Medical Center, Duarte, CA; National Center for Toxicological Research, Jefferson, AR; Northwestern University medical School, Chicago, IL.

Background: Mitochondria are dynamic organelles that play critical roles in oxidative phosphorylation and energy metabolism. Mitochondrial DNA damage and dysfunction play vital roles in the development of a wide array of mitochondria-related diseases, such as obesity, diabetes, infertility, and malignant tumors in human. Here, we reported the generation of a transgenic (TG) mouse model of human mitochondrial diseases by overexpressing hOGG1, a base excision DNA repair gene, in the mitochondria of a wide variety of tissues in mice.

Design: hOGG1 TG mice were produced by pronuclear microinjection using a mammalian expression vector consisting of a mitochondrial isoform of the human OGG1 full-length cDNA under the regulation of mouse metallothionein promoter 1 (mMT-1). Transgene integration was analyzed by PCR. Gene expression was measured by real-time RT-PCR and western blot analysis. Mitochondrial DNA damages were analyzed by direct DNA sequencing and real-time quantitation of mitochondrial copy number. Total fat content was measured by whole body scan using Dual Energy X-ray Absorbtiometry.

Results: The hOGG1 TG mice express very high levels of human OGG mRNA (50 to 1000 folds as high as endogenous mouse OGG) in almost all organs analyzed with the liver being the highest expressing organ. Significantly more mitochondrial DNA mutations and less mitochondrial copies per cell were seen in hOGG1 TG mice. hOGG1 TG mice become obese from 2 months of age as manifested by increased body weight and whole body fat percentage. Diffuse steatosis develops progressively with age. The female TG mice are infertile. At about 2 years of age, increased frequencies of hematopoeitic malignancies are seen in these TG mice.

Conclusions: Defects in mitochondrial genome and function have profound adverse biological effects in mice, resulting in obesity, hepatosteatosis, female infertility and the development of hematopoeitic malignancies, presumably brought about by the disruption of energy and fatty acid metabolism and increased ROS production.

1377 Mitochondrial DNA Damages Enhance the Cell Killing Effects of Cisplatin in Human Hepatoma Cells *Via* Increased Intracellular Free Radical Production

H Zhang, J Trullols, M Higuchi, BR Smoller, CY Fan. University of Arkansas for Medical Sciences, Little Rock, AR.

Background: Cancer cells are constantly under oxidative stress and susceptible to free radical-induced apoptosis. Defect in mitochondrial respiration has been shown to cause increased free radical production and, consequently, enhanced sensitivity to apoptosis-induced chemotherapeutic agent in cancer cells. Overexpression of base excision repair gene in cells will cause imbalance in base excision repair, leading to paradoxically increased DNA breakages. In this study, we explore a novel strategy of enhancing cell killing effect in human hepatoma cells by Cisplatin by overexpression of hOGG1, a base excision DNA repair gene in the mitochondria of a human hepatoma cell line.

Design: The mitochondrial isoform (2a) of hOGG1 gene was overexpressed in a human hepatoma cell line (HepG2). The expression of mMT-hOGG1 transgene was measured by RT-PCR and fluorescent immunohistochemistry. Mitochondrial DNA deletion was analyzed by long-range PCR. The amount of free radicals (hydrogen peroxide and superoxide) was measured by flow cytometric analysis. Apoptosis was measured by flow cytometric analysis. Responses to chemotherapy (Cisplatin) in these cells were determined by colony formation experiments.

Results: mMT-hOGG1 transfected hepatoma cells (H8) expressed high levels of transgene mRNA as compared to the control cells by RT-PCR and the protein product of the expressed transgene was targeted successfully to the mitochondria in H8 hepatoma cells by fluorescent immunohistochemistry. There were much enhanced mitochondrial DNA deletions and production of free radicals (hydrogen peroxide and superoxide) in the H8 cells as compared to the control hepatoma cells. H8 hepatoma cells underwent more active apoptosis and consequently, more susceptible to the cell killing effects of Cisplatin, a common chemotherapeutic agent used in the treatment of liver cancer.

Conclusions: Targeting of hOGG1 gene expression to the mitochondria in human hepatoma cells increases the sensitivity of cancer cells to the killing effects of Cisplatin through enhanced mitochondrial DNA deletions, production of free radicals, and increased intrinsic apoptosis. The violation of mitochondrial DNA integrity or disruption of its function, thus represents a novel mechanism upon which more effective chemotherapeutic strategies can be developed in the treatment of human cancer.

1378 Cell Surface Molecule R9.14 Is Expressed by Monoblastic Leukemia of FAB M5 Type as Well as Reed-Sternberg Cell Lines and Anaplastic Large Cell Lymphoma Cell Lines

M Zhou, FM Fadl El Mola, H Chang, J Cohn, R Karim, D Hogge, D Banerjee. British Columbia Cancer Agency, Vancouver, BC, Canada; Prince Margaret Hospital, Toronto, ON, Canada; Ontario Cancer Institute, Toronto, ON, Canada; British Columbia Cancer Research Centre, Vancouver, BC, Canada.

Background: Anti-R9.14 is a murine monoclonal antibody raised in the Banerjee laboratory against KMH-2 cells, a Hodgkin lymphoma-derived cell line. During testing of the specificity of the antibody, it was observed that, unlike all other antibodies raised against KMH-2 cells, anti-R9.14 labelled not only CD30+ Hodgkin and Anaplastic Large Cell lymphoma cell lines, but also labelled a CD30 negative monoblastic cell line U937. This led to the investigation of the expression of R9.14 on leukaemic blasts from patients with newly diagnosed acute myeloid leukemia (AML).

Design: Antigen expression was studied by flow cytometry and the antigen is further identified with Western-blot analysis.

Results: Of 16 AML patients studied by flow cytometry, the CD45 dim blast cells expressing R9.14 were determined to be only in patients with acute monoblastic leukemia (AMoL) of both FAB M5a and FAB M5b categories. Blast cells of other FAB types did not express the epitope. R9.14 is also expressed by monocytes but not normal CD34+ bone marrow precursors, granulocytes, lymphocytes or erythroid precursors. By Western blot analysis R9.14 is a ~92 KDa molecule. Anti-R9.14 has a pleiotropic effect on cell proliferation, depending upon the cell line and the incubation time.

Conclusions: R9.14 may be functionally significant in monoblastic leukemia, Hodgkin lymphoma and Anaplastic Large Cell Lymphoma. Molecular cloning and sequencing of the R9.14 gene will be undertaken.

Pediatrics

1379 Portal Vein Alterations in Patients with Extrahepatic Biliary Atresia

JE Acosta, FG Varela, MP Valencia. Hospital Infantil de Mexico, Mexico, DF, Mexico.

Background: Vascular lesions of the liver are protean and may be observed in several conditions; **arterial** lesions have been observed in extrahepatic biliary atresia (EBA). Alterations of the portal **vein** or its main branches, to our knowledge, have not previously been described. Peculiar portal vein lesions found in a group of patients with EBA are here informed.

Design: This is a descriptive, retrospective study of 62 consecutive biopsies of patients with EBA who underwent porto-biliary anastomosis, in a ten years period. Vessels from the hepatic hilium were studied with H & E, Masson´s trichrome, elastic fibers, mucicarmin, alcian blue, PAS, coloidal iron, CD20, CD3, CD68, and actin stains. Celular or fibrous subendothelial proliferation, elastica damage, edema, calcification, thrombosis, and glycosaminoglycan deposits were searched; the extention of the damage was graded as mild (less than 25% of circumference), moderate (26 to 50%), or severe (over 50%). Vessels were classified according to their circumference as medium sized (less than 300 microns) and large; when possible the portal vein and/or its larger branches were evaluated. Hepatic explants (n=20) of patients without EBA were used as controls. Demographic data were obtained from clinical charts.

Results: Age averaged 3 months; 45 patients were females. In 24 cases portal vein or its larger branches were present. Vascular alterations were observed in 35 cases: arterial changes in 13, vein lesions in 10, and damage in both types of vessels in 12. The main arterial changes found were: elastica rupture (n=19), glycosaminoglycans deposits(n=19), and subendothelial celular proliferation (n=20); all changes were mild to moderate. On the other hand, glycosaminoglycans deposits (n=7), subendothelial fibrous proliferation (n=8), and elastic fibers rupture (n=9), were the principal alterations observed in the portal vein or its branches; all changes were mild.Subendothelial